Microarray-Assisted Pathway Analysis Identifies Mitogen-Activated Protein Kinase Signaling as a Mediator of Resistance to the Green Tea Polyphenol Epigallocatechin 3-Gallate in Her-2/neu–Overexpressing Breast Cancer Cells

Shangqin Guo,[1] Jun Lu,[2] Aravind Subramanian,[2] and Gail E. Sonenshein[1]

[1]Department of Biochemistry and Women's Health Interdisciplinary Research Center, Boston University School of Medicine, Boston, Massachusetts and [2]Broad Institute of Massachusetts Institute of Technology and Harvard, Cambridge, Massachusetts

Abstract

Overexpression of the epidermal growth factor receptor family member Her-2/neu in breast cancer leads to autophosphorylation of the receptor and induction of multiple downstream signaling pathways, including the Akt kinase to nuclear factor-κB (NF-κB) cascade that is associated with poor prognosis. Previously, we showed that the green tea polyphenol epigallocatechin 3-gallate (EGCG) inhibits growth of NF639 Her-2/neu–driven breast cancer cells via reducing receptor autophosphorylation and downstream Akt and NF-κB activities. Interestingly, upon prolonged culture in the presence of EGCG, cells resistant to the polyphenol could be isolated. Here, we report that resistant cells have lost tyrosine phosphorylation on the Her-2/neu receptor. Surprisingly, they displayed elevated NF-κB activity, and inhibition of this activity sensitized cells to EGCG. Data from microarray studies of the original and resistant NF639 populations of cells were subjected to Gene Set Enrichment Analysis pathway assessment, which revealed that the mitogen activated protein kinase (MAPK) pathway was activated in the resistant cells. Treatment of the resistant cells with the MAPK inhibitor U0216 reduced growth in soft agar and invasive phenotype, whereas the combination of EGCG and U0216 resulted in cells with a cobblestone epithelial phenotype. Thus, activation of the MAPK pathway mediates resistance to EGCG. (Cancer Res 2006; 66(10): 5322-9)

Introduction

The *Her-2/neu* (or *c-erbB-2*) oncogene, the second member of the epidermal growth factor (EGF) receptor family (EGFR-2), encodes a transmembrane receptor tyrosine kinase. Overexpression of Her-2/neu, which has been seen in ~30% of human breast cancers, is associated with poor prognosis and overall patient survival (1). In particular, Her-2/neu overexpression in breast cancers has been found associated with increased metastatic potential (2). Transgenic mice overexpressing Her-2/neu develop mammary tumors (3). Activation of overexpressed Her-2/neu via autophosphorylation induces multiple downstream signaling pathways, e.g., phosphatidylinositol 3-kinase (PI3K) to serine/threonine kinase Akt/protein kinase B to NF-κB (4). Signaling from the Her-2/neu/PI3K/Akt pathway confers resistance to antihormones (5) and chemotherapeutic drugs (6). Activation of NF-κB through Her-2/neu/PI3K/Akt has been well established (7). Aberrant activation of various NF-κB subunits is prevalent in human breast cancer specimens (8). Overexpression of the c-Rel NF-κB subunit induces mammary tumor formation in mice (9). Importantly, activated NF-κB provides crucial survival signals, protecting many malignant cells from apoptosis induced by various chemotherapeutic agents (10, 11), and thus inhibition of NF-κB potentiates their killing (12, 13). Her-2/neu has been an attractive therapeutic target for malignant diseases that overexpress this receptor. Trastuzumab, a humanized monoclonal antibody against Her-2/neu, has important activity against Her-2/neu–positive metastatic breast cancers (14). Small molecule tyrosine kinase inhibitors, such as Iressa/ZD1839/Gefitinib and GW572016, are another class of drugs targeting the EGF family receptors. However, it is not uncommon that resistance to these drugs develops after an initial response (14–17) via diverse mechanisms (16–18).

Green tea, which is rich in polyphenols such as epigallocatechin-3 gallate (EGCG), has anticarcinogenic activity against a variety of tumor types, including breast cancer (19, 20). For example, we showed that female rats given green tea as their drinking fluid displayed a significant decrease in carcinogen-induced mammary tumor burden and invasive phenotype with significantly increased latency to first tumor (21). More recently, we showed that EGCG treatment of Her-2/neu–overexpressing mammary tumor cells reduced their rate of proliferation, ability to grow in soft agar, tyrosine phosphorylation of the Her-2/neu receptor, and Akt to NF-κB signaling pathway (22). Interestingly, we noted that some of the NF639 Her-2/neu–driven mouse mammary tumor cells showed resistance to EGCG-mediated inhibition, e.g., they continued to grow in soft agar. Here, we have characterized EGCG-resistant NF639 breast cancer cells to model rational design of combinatorial drug therapy. Compared with EGCG-sensitive cells, resistant cells displayed a loss of Her-2/neu receptor tyrosine autophosphorylation and a higher constitutive NF-κB activity, which was required for resistance. Signaling pathway and biochemical analyses of gene expression profiling identified a role of elevated mitogen activated protein kinase (MAPK) signaling in EGCG resistance.

Materials and Methods

Cell growth and treatment conditions. The NF639 cell line (kindly provided by P. Leder, Harvard Medical School, Boston, MA) was derived from a mammary gland tumor in a mouse mammary tumor virus-*Her-2/neu* mouse (23). These cells, which display high constitutive Her-2/neu tyrosine phosphorylation, were maintained in complete medium (DMEM

Requests for reprints: Gail E. Sonenshein, Department of Biochemistry, Boston University School of Medicine, 715 Albany Street, Boston, MA 02118. Phone: 617-638-4120; Fax: 617-638-4252; E-mail: gsonensh@bu.edu.

doi:10.1158/0008-5472.CAN-05-4287

supplemented with 10% fetal bovine serum, and antibiotics), as described previously (22). EGCG, purchased from LKT Laboratories, Inc. (St. Paul, MN), was dissolved in sterile DMSO. Dexamethasone and the MAPK inhibitor U0216 were purchased from Sigma (St. Louis, MO) and Cell Signaling (Danvers, MA), respectively.

Focus formation assay and colony recovery. NF639 cells were plated in triplicate at 7.5×10^3/mL in top plugs consisting of complete medium and 0.8% SeaPlaque agarose (FMC Bioproducts, Rockland, ME) with the indicated concentration of EGCG, whereas the equivalent amount of DMSO for the highest EGCG dose was used as control. Plates were subsequently incubated for 2 weeks in a humidified CO_2 incubator at 37°C. Cells were stained with 2 mL crystal violet solution, washed, and colonies were counted using an inverted bright field microscope at a ×2 magnification. Three random fields were counted from each of the triplicate samples, and average of the nine values were presented ± SD, which was obtained using the Student's *t* test. To recover a pool of colonies that survived EGCG treatment, 1 to 2 mL complete medium was added and following gentle pipetting, cells were transferred to a fresh tissue culture dish containing complete medium. Single colonies were established by serial dilution.

Matrigel assay. Matrigel (BD Biosciences, San Jose, CA) was diluted with cold serum-free DMEM to a working concentration of 6.3 mg/mL and kept on ice till use. Samples (200 μL) were added to wells of a 24-well dish, which was subsequently incubated at 37°C for 30 minutes to allow the Matrigel to solidify. Single cell suspensions (10 μL) containing 5×10^3 NF639 cells were then mixed with 190 μL Matrigel at 4°C and added to the preset Matrigel layer. Following incubation at 37°C for 30 minutes, 500 μL complete growth medium was layered on top and the dishes were incubated for 3 to 7 days. Colonies were photographed using a Zeiss Axiovert 200 M microscope.

Electrophoretic mobility shift assay. Nuclear extracts were prepared from breast cancer cells in extraction buffer [420 mmol/L KCl, 20 mmol/L HEPES (pH 7.9), 1.5 mmol/L $MgCl_2$, 0.2 mmol/L EDTA, and 20% glycerol] plus protease inhibitors [0.5 mmol/L DTT, 0.5 mmol/L phenylmethylsulfonyl fluoride (PMSF), and 10 μg/mL leupeptin], as we have published previously (7). The sequence of the URE NF-κB-containing oligonucleotide from the c-*myc* gene is as follows: 5′-GATCCAAGTCCG**GG**TTTTCCCCCAACC-3′, where the underlined region indicates the core binding element. The mutant URE has a 2 bp transversion of G residues (indicated in bold) to C residues, which greatly reduces NF-κB binding. The sequence of the Sp1 oligonucleotide is 5′-ATTCGATCGGGGCGGGGCGACC-3′. The sequence of the Oct-1 oligonucleotide is 5′-TGTCGAATGCAAATCACTAGAA-3′. Oligonucleotides were end labeled with large Klenow fragment of DNA polymerase and [^{32}P]deoxynucleotide triphosphates. The electrophoretic mobility shift assays (EMSA) were done using 5 μg nuclear extract, as we have published previously (7).

Transfection analysis. The original and resistant pools of NF639 cells were transfected, in triplicate, with a choloramphenicol acetyl transferase (CAT) reporter construct driven by two copies of either wild-type URE NF-κB element (E8) or mutant NF-κB element (dmE8; ref. 24). Forty-eight hours after transfection, cells were harvested and processed for CAT assay as described previously (25). CAT activity was normalized to protein content and is presented as mean values of the triplicate samples ± SD.

Immunoblot analysis. Cells were rinsed with cold PBS and harvested in lysis buffer [50 mmol/L Tris-HCl (pH 8.0), 5 mmol/L EDTA (pH 8.0), 150 mmol/L NaCl, 0.5 mmol/L DTT, 2 μg/mL aprotinin, 2 μg/mL leupeptin, 0.5 mmol/L PMSF, and 0.5% NP40]. Whole cell extracts were obtained by sonication, followed by centrifugation at 14,000 rpm for 30 minutes. Samples (30-50 μg) were subjected to electrophoresis in an 8% or 10% polyacrylamide-SDS gel and immunoblot analysis, as previously described (7). Antibodies used were as follows: phosphotyrosine (Santa Cruz Biotechnology, Santa Cruz, CA), neu, IκB-α, extracellular signal-regulated kinase (ERK; Cell Signaling), phospho-ERK (Cell Signaling), and β-actin (Sigma).

Microarray and computational analyses. Total RNA of original NF639 cells and EGCG-resistant NF639 cells from two independent experiments were harvested using the UltraspecII RNA isolation kit (Biotecx, Houston, TX), following the instructions of the manufacturer. Samples were profiled for mRNA expression using Affymetrix Mouse 430A 2.0 chips at Boston University Microarray Resource. Data were subjected to the Gene Set Enrichment Analysis (GSEA; ref. 26), using the March 2005 build of gene set collection. *P* values were calculated through permuting gene labels, using weighed gene set enrichment score. The gene expression data have been deposited in the GEO database.[3]

Results

Loss of Her-2/neu receptor tyrosine phosphorylation in EGCG-resistant cells. Although growth of the Her-2/neu–driven NF639 cells in soft agar was inhibited in a dose-dependent fashion by EGCG (22), some cells seemed to display increased resistance to treatment. Thus, ~65% of colony formation was inhibited at 40 μg/mL EGCG, and 95% at 80 μg/mL EGCG; however, 5% of the colonies remained even at this elevated dose. To assess the mechanism of resistance, we isolated 18 individual colonies (termed clones 1-18) and a pool of colonies that grew in the presence of 40 μg/mL EGCG for 2 weeks. Because EGCG treatment significantly decreased receptor autophosphorylation in the original population of cells (22), we first tested the basal level of Her-2/neu receptor tyrosine phosphorylation in the clones. Whole cell extracts were prepared from each clone and the original population, and samples were subjected to immunoblot analysis using an antiphosphotyrosine antibody, which recognizes a previously characterized band corresponding to the 185 kDa Her-2/neu receptor (7). Three of 18 clones (clones 11, 17, and 18) displayed levels of activated Her-2/neu similar to that of the original population, whereas the other 15 clones showed only residual tyrosine phosphorylation on the Her-2/neu receptor, indicating that EGCG favored selection of phospho-Her-2/neu–negative cells (Fig. 1*A*). The absence of phosphorylated Her-2/neu in the resistant cells did not seem due to loss of Her-2/neu transgene expression, as judged by reprobing of the same blot with an antibody that recognizes both phosphorylated and unphosphorylated Her-2/neu protein. Her-2/neu protein expression was detected in all of the clones (Fig. 1*A*). The three clones (clones 11, 17, and 18) that were positive for tyrosine-phosphorylated Her-2/neu displayed a slower migrating band with the antibody recognizing total Her-2/neu, consistent with migration of a phosphorylated neu protein (Fig. 1*A*). The blot was also probed for β-actin to control for equal protein loading (Fig. 1*A*). Although some variability was noted, the difference in Her-2/neu protein expression could not account for the loss of phosphorylated Her-2/neu in most of the clones. In addition, when mixed cultures of original and resistant populations were compared, a reduced level of phospho-Her-2/neu was again observed similar to that seen with many of the clones (data not shown).

To test for their sensitivity toward EGCG, clones 11 and 17 (expressing high levels of phospho-Her-2/neu) and clones 5 and 12 (expressing low levels of phospho-Her-2/neu) were grown in soft agar in the presence of 40 μg/mL EGCG (Fig. 1*B*). As control, plates with the original population of cells were similarly analyzed. EGCG inhibited growth of clones 11 and 17 to an extent essentially equivalent to the original population. Similar data was obtained with clone 18 (data not shown). In contrast, substantial growth of clones 5 and 12 was observed in the presence of 40 μg/mL EGCG. Moreover, clones 5 and 12 grew quite aggressively in the absence of EGCG, with colonies appearing very spread out,

[3] Results are deposited at www.ncbi.nlm.nih.gov/geo/.

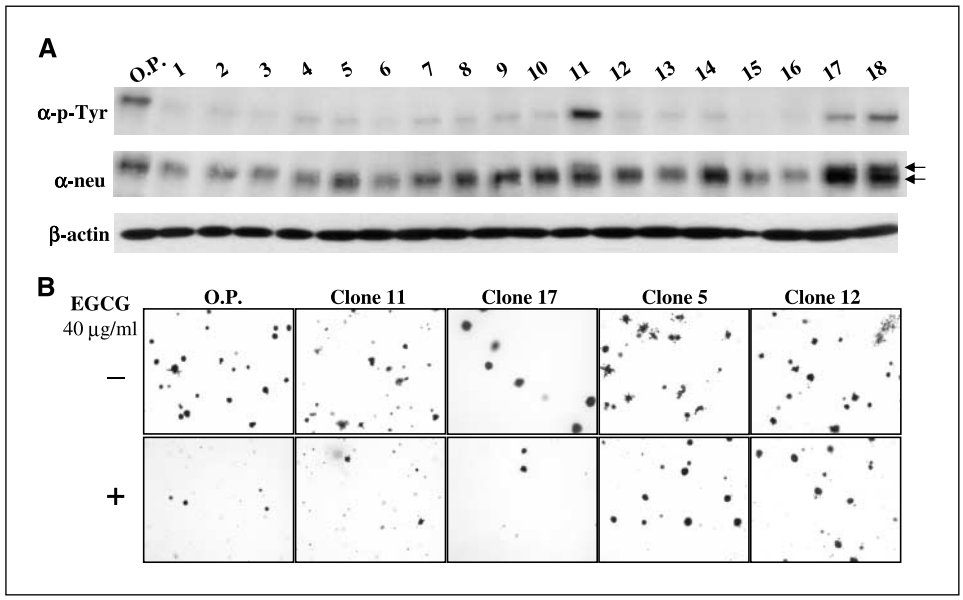

Figure 1. EGCG-resistant cells have lost tyrosine phosphorylation on the Her-2/neu receptor. *A,* whole cell extracts were prepared from each of the 18 EGCG-resistant clones, as well as the original population of cells (*O.P.*), and resolved on an 8% SDS-PAGE. The gel was then processed for immunoblotting using an antibody recognizing the tyrosine phosphorylated Her-2/neu receptor (*α-p-Tyr*). The same blot was then reprobed using an antibody recognizing the neu protein, either phosphorylated or nonphosphorylated (*α-neu*). Western blot for β-actin confirmed essentially equal protein loading. The reduced expression of phospho-Her-2/neu was seen even after 3 weeks in culture in the absence of EGCG (data not shown). *B,* the original population of NF639 cells, and clones 11, 17, 5, and 12 (described above) were grown in soft agar in the presence of 40 μg/mL EGCG (+) or equivalent amount of carrier DMSO solution (−). Representative fields from each clone or the original population are shown.

suggesting a more malignant phenotype (Fig. 1*B*). Similar data was obtained with clones 2 and 7 (data not shown). Taken together, our data suggest that the loss of Her-2/neu tyrosine phosphorylation was common in the resistant cells, which provided a mechanism by which they evaded EGCG-mediated growth inhibition.

EGCG-resistant cells display elevated levels of NF-κB activity. Previously, we showed that the activation of p65/p50 and p50/p50 NF-κB complexes, which is mediated through Her-2/neu/PI3K/Akt signaling (7, 27, 28), is reduced by EGCG treatment of the original population of NF639 cells via inhibition of the autophosphorylation that initiates the cascade (22). Thus, we next examined NF-κB binding activity in the clones. EMSA was done using oligonucleotides containing the NF-κB element upstream of the c-*myc* oncogene promoter (24) or an Sp-1 element as control (Fig. 2*A*; ref. 7). NF-κB binding was detected in all of the clones. Interestingly, the level of binding was substantially lower in clones 11, 17, and 18, which displayed phosphorylated Her-2/neu and sensitivity to EGCG (Fig. 1). Nine of the remaining 15 clones displayed elevated NF-κB levels compared with the original population. Of note, clones 5 and 12 expressed extremely high levels of NF-κB nuclear binding compared with the original population.

To confirm that the reduced level of phospho-Her-2/neu and increased NF-κB activity was a common property of EGCG-resistant cells rather than an issue of clonal variation, mixed cultures of original and resistant populations were subjected to transfection analysis using reporter vectors driven by two copies of either wild-type or mutant NF-κB elements (E8-CAT and dmE8-CAT, respectively; Fig. 2*B*; ref. 24). The dmE8-CAT gave comparable activity in both the original and resistant populations of cells, suggesting their capabilities to take up plasmid DNA were similar. E8-CAT displayed almost 2-fold higher activity in the resistant cells compared with the original population (Fig. 2*B*). Similar results were obtained using luciferase reporter driven by three tandem NF-κB sites from MHC class I promoter (data not shown; ref. 29). Collectively, these data suggest that NF-κB activity was elevated in the resistant cells independent of Her-2/neu receptor tyrosine phosphorylation.

Reduction in NF-κB activity sensitizes cells to EGCG-mediated growth inhibition. To test the role of NF-κB in resistance to EGCG-mediated inhibition of growth in soft agar, the original population of NF639 cells were infected with a retrovirus expressing human IκBα, the specific inhibitor of NF-κB. EMSA of nuclear extracts from these cells indicated that IκBα expression resulted in a large decrease in the binding of p65/p50 NF-κB heterodimers and only a modest reduction in p50 homodimer complexes, consistent with its known preference for p65 versus p50 subunits (Fig. 2*C*; ref. 30). The ectopic expression of human IκBα protein was confirmed by immunoblot analysis using an antibody that recognizes both human and mouse IκBα (Fig. 2*D, inset*). Expression of IκBα substantially reduced the ability of colonies to grow in the presence of 40 μg/mL EGCG (Fig. 2*D*). In the absence of IκBα, colony formation was decreased to ~35% of control values by EGCG, whereas only 15% of control colony numbers were detected with the combination of EGCG and IκBα. These data indicate that NF-κB activity plays an essential role for growth in soft agar in the presence of EGCG, consistent with our previous findings (22, 31).

Dexamethasone inhibits anchorage-independent growth of EGCG-resistant cells. The glucocorticoid receptor ligand dexamethasone is known to potently inhibit NF-κB activity (32). The effects of addition of dexamethasone and EGCG alone or in combination on the ability of the resistant cells to grow in soft agar were tested. Addition of the solvent carriers (DMSO and ethanol) had minimal effects on growth in soft agar of either the original NF639 cells or the resistant pool cells (Fig. 3, *control lanes*) or growth on culture plates (data not shown). Again, the resistant cells gave rise to larger colonies. Treatment with 40 μg/mL EGCG had minimal effect on resistant cells, whereas colony formation by the original population was largely inhibited. When cultures were treated with 20 μmol/L dexamethasone alone, a reduction in colony size was observed with both populations without much effect on colony numbers. When both EGCG and dexamethasone were added, almost all the colony-forming ability was inhibited in the resistant cells, as well as the original population. These data confirm additive effects of EGCG and dexamethasone.

Microarray analysis identifies activation of the MAPK pathway in EGCG-resistant cells. To more systematically reveal the mechanisms of EGCG resistance, we used a microarray

approach to identify signaling pathways that have been altered in EGCG-resistant cells. The mRNA expression profiles were generated from two independent experiments.[3] The expression of a large number of genes was changed in the resistant cells compared with the original population. However, none of our analysis of individual genes could provide a mechanistic explanation for the observed resistance (see Discussion). Thus, the data were subjected to GSEA (26), which was designed to determine whether a defined set of genes displays a statistically significant, concordant difference between two biological states. The analysis retrieved gene sets that were enriched in either the original or resistant NF639 cells. The top 10 gene sets with the smallest nominal *P* values enriched in either cell type were obtained. Two independently annotated MAPK gene sets were identified within the top 10 list for the resistant cells (Table 1), which made it less likely that the scoring was a result of poor curation of the gene sets. Given the evidence for a critical role in the regulation of tumor cell migration and metastasis (reviewed in ref. 33), the functional status of the MAPK pathways in the resistant cells was further examined. Whole cell extracts from the EGCG-resistant and original NF639 populations of cells were probed for active, phosphorylated ERK and c-Jun (Fig. 4*A*). An elevated level of phospho-ERK was detected in the resistant versus the original population of cells. In contrast, when the total ERK protein was measured, reduced protein expression was seen in the resistant cells, likely due to an enhanced rate of ubiquitination and proteasome-mediated degradation seen with the phosphorylated proteins (34). Additionally, the level of phosphorylated c-Jun, an indicator of the activated c-Jun-NH_2-kinase (JNK) pathway, as well as the total c-Jun, was also increased in the resistant cells. The elevated levels of phospho-ERK and phospho-c-Jun confirmed that the MAPK pathway was indeed activated in the resistant cells.

Consistent with the finding that Her-2/neu autophosphorylation was reduced in EGCG-resistant cells, the Akt pathway, which is downstream of Her-2/neu signaling, ranked among the top 10 gene sets that are enriched in the original cell population compared with the resistant cells (data not shown). Indeed, Western blot analyses confirmed that the Akt kinase seemed to be reduced in the resistant cells at both protein and phosphorylation levels (Fig. 4*A*). Thus, the sensitive population shows high Akt, whereas the resistant population displays elevated ERK activity.

MAPK inhibitor U0216 reverses mesenchymal phenotype of the resistant cells. To assess whether the elevated MAPK activity is functionally important for EGCG resistance, the original and resistant NF639 cell populations were grown in soft agar in the presence of 10, 20, or 30 μmol/L U0216 MAPK inhibitor, or control DMSO carrier solution. Whereas little change in colony size was seen with the original population upon treatment with 10 μmol/L U0216, a substantial decrease in size of colonies of the resistant cells was observed (Fig. 4*B*). Of note, treatment with 30 μmol/L U0216 resulted in colonies of resistant cells that were smaller than those of similarly treated original population of NF639 cells (Fig. 4*B*). Immunoblot analysis for phospho-ERK confirmed that U0216 effectively inhibited MAPK activity in NF639 cells (Fig. 5*B, inset*). The ERK pathway, induced by Her-2/neu signaling, has been implicated in promoting invasive potential of cancer cells (35, 36). Thus, we next tested the effects of U0216 on colony formation in Matrigel. The original and resistant NF639 cells were plated in

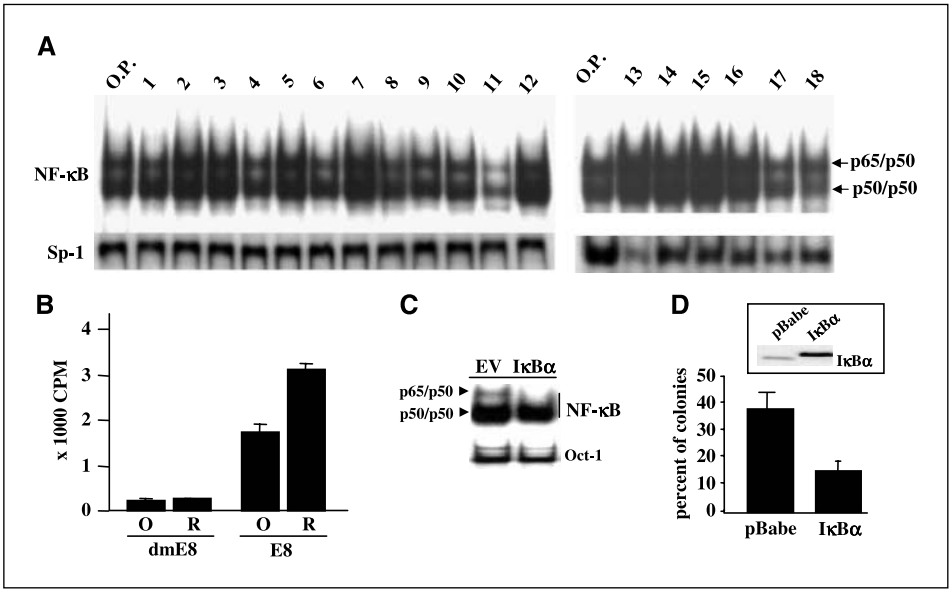

Figure 2. Inhibition of elevated NF-κB activity in resistant cells leads to enhanced sensitivity to EGCG. *A,* samples of nuclear extracts (5 μg) from the original population of NF639 cells and the 18 clones described in Fig. 1 were subjected to EMSA using as probes oligonucleotides containing either the NF-κB element from the c-*myc* promoter (*top*) or Sp-1 (*bottom*) as loading control. The samples were run on two gels. Thus, to be able to compare binding between gels, the same extract from the original population was used for normalization. The positions of p65/p50 and p50/p50 NF-κB complexes are shown based on previous supershift EMSA data (10). *B,* the original (*O*) and resistant pools (*R*) of NF639 cells were transfected, in triplicate, with a reporter CAT construct driven by two copies of either mutant (*dmE8*) or wild-type (*E8*) NF-κB elements. Forty-eight hours after transfection, CAT activity was determined. *Columns,* mean values normalized to protein content; *bars,* SD. *C* to *D,* NF639 cells were infected with an empty pBabe retrovirus (*EV*) or one expressing human IκBα and nuclear and whole cell extracts prepared. *C,* samples (5 μg) of nuclear extracts were subjected to EMSA for NF-κB or Octomer-1 (*Oct-1*), as control for equal protein loading. *D,* cultures of the pBabe- and IκBα-expressing NF639 cells were grown in soft agar in the absence or presence of 40 μg/mL EGCG and the colonies were counted. The number of colonies grown in the presence of EGCG were normalized to that in the absence of EGCG, which was set as 100%. *Inset,* Western blot analysis was done on samples of whole cell extracts (30 μg) using an antibody that recognizes both the murine and human forms of IκBα, confirming the expression of the human IκBα.

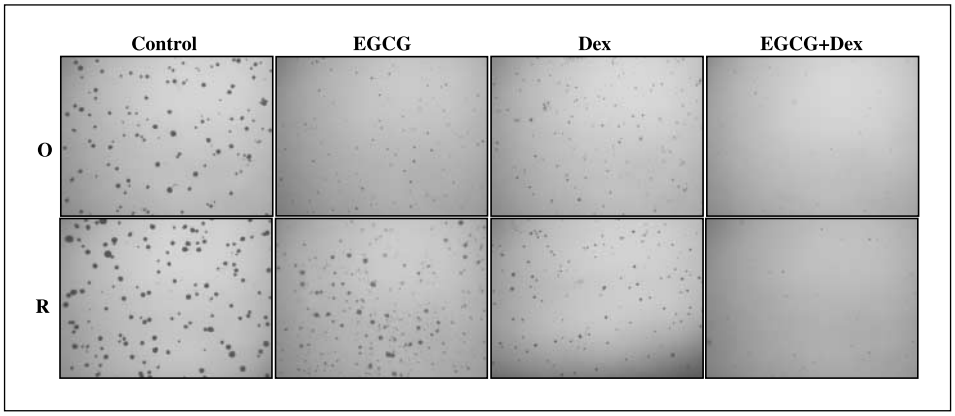

Figure 3. Dexamethasone and EGCG cooperate to inhibit anchorage-independent growth of resistant cells. The original population and resistant pools of NF639 cells were grown in soft agar in the presence of either 40 μg/mL EGCG or 20 μmol/L dexamethasone (*Dex*) alone or in combination, or with equivalent amount of control carrier solution (DMSO and ethanol, respectively). Representative fields for each condition are shown.

Matrigel in the presence of 5, 10, or 30 μmol/L U0216 or control carrier solution DMSO and grown for 6 days. In the absence of U0216, the original and resistant cells gave extensive branched structures, although the size of the colonies seemed somewhat larger with the resistant cells, consistent with the growth in soft agar (Fig. 4*C*). When grown in the presence of 5 or 10 μmol/L U0216, a pronounced inhibition of branching and reduction in colony size was noted with the resistant cells, whereas branching colony formation of original NF639 cells was largely unaffected. Similar data were obtained with growth in soft agar (data not shown). Thus, resistant cells display elevated MAPK activity and inhibition of this activity with U0216 reduces their mesenchymal, invasive phenotype.

We next tested the effects of combined treatment of EGCG and inhibition of MAPK signaling on cell morphology. The original and resistant populations of cells were treated in culture with 20 μmol/L U0216 or 40 μg/mL EGCG alone or in combination for 72 hours and the cells analyzed. When grown in the presence of control carrier DMSO, both populations of cells failed to contact inhibit after reaching confluence, forming multilayers (Fig. 5). Addition of U0216 alone had a more profound effect on the resistant cells, whereas the original population of cells responded to EGCG treatment displaying a more flattened appearance. When EGCG and U0216 were combined, a dramatic change in appearance of the resistant cells was noted. The cells assumed a more cobblestone epithelial appearance and the cells grew to confluence as a monolayer, consistent with the Matrigel analysis.

Discussion

Here, we show that Her-2/neu–transformed breast cancer cells resistant to EGCG are highly invasive and display elevated MAPK signaling and enhanced activation of NF-κB. EGCG-resistant cells also show reduced tyrosine phosphorylation of the Her-2/neu receptor and Akt activation. Inhibition of NF-κB via ectopic expression of IκBα reduced the resistance to EGCG. Furthermore, combined treatment with EGCG and dexamethasone, which is a

Table 1. Top 10 gene sets enriched in the EGCG-resistant NF639 cells

Gene set name	Nominal *P*	Brief description
DOWN_G1ER	0	Genes down-regulated in G1E-ER4 GATA-1-null erythroblast cells
ADULT_LIVER_vs_FETAL_LIVER_GNF2	0	Genes up-regulated in adult liver vs fetal liver
HTERT_DOWN	0	Genes down-regulated by telomerase
IVANOVA_STEMNESS	0.035	Genes that define stem cell identity
p35Alzheimers' Pathway	0.036	p35 cleaved to p25 that promotes τ hyperphosphorylation and apoptosis and is implicated in Alzheimer's disease
CR_SIGNALLING	0.049	Cancer-related genes involved in cell signaling
MAPK_Cascade	0.053	Genes part of the MAPK signaling cascade
ST_JNK_MAPK_Pathway	0.054	JNKs are MAPKs regulated by several levels of kinases (MAPKK, MAPKKK) and phosphorylate transcription factors and regulatory proteins
CR_IMMUNE_FUNCTION	0.063	Cancer-related genes involved in immune function
INS	0.065	Genes related to insulin signaling

NOTE: Gene expression data from EGCG-resistant or original populations of NF639 cells were obtained on Affymetrix Mouse 430A 2.0 chips and were subjected to GSEA analysis using the March 2005 build of gene set collection. Nominal *P* values were calculated based on weighed gene set enrichment score and by permuting gene labels. Gene sets that are enriched in resistant population compared with original population were sorted according to nominal *P* values. The top 10 gene sets are shown.

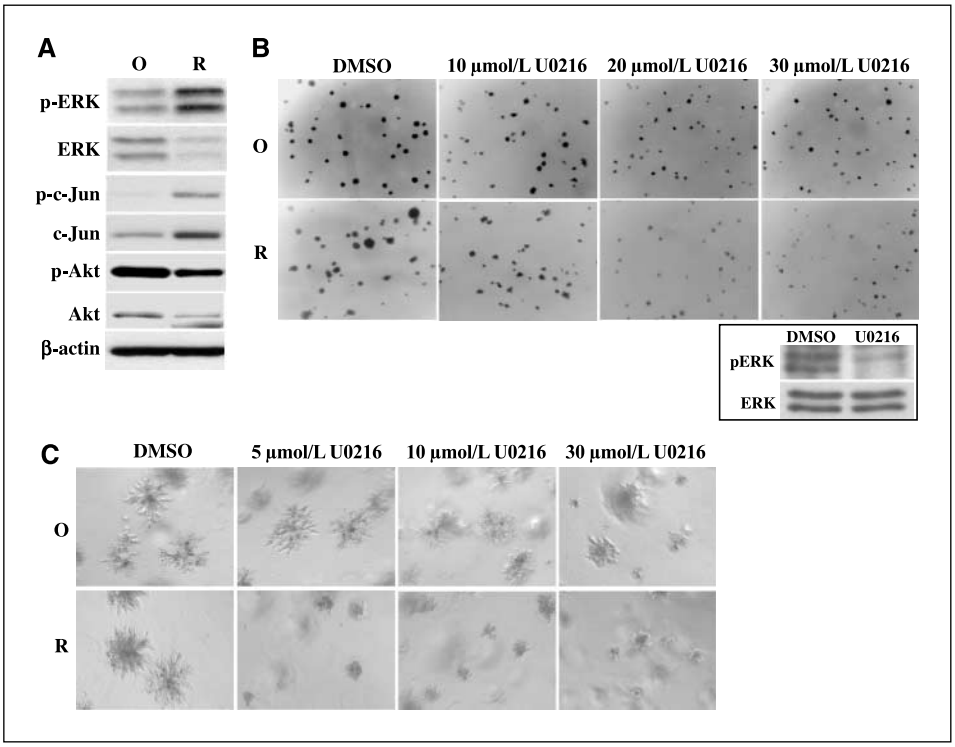

Figure 4. Resistant cells display elevated levels of MAPK activation. *A,* whole cell extracts were prepared from original and EGCG-resistant populations of NF639 cells grown in medium containing 0.5% fetal bovine serum for 48 hours. Samples (30 μg) were analyzed by immunoblotting for phosphorylated and total levels of ERK, c-Jun, and Akt. Blotting for β-actin controlled for equal protein loading. *B,* original and resistant populations of NF639 cells were plated in soft agar in the presence of 10, 20, or 30 μmol/L U0216 MAPK inhibitor or equivalent carrier solution DMSO for 2 weeks, and representative fields were photographed. *Inset,* the original population of NF639 cells was treated with 30 μmol/L U0216 for 1 hour and whole cell extracts (30 μg) were analyzed for the expression of phospho-ERK and total ERK. *C,* original and resistant populations of cells (5,000) were plated into Matrigel and grown for 6 days in the presence of 5, 10, or 30 μmol/L U0216 or carrier solution DMSO, as control. Representative fields are shown.

potent inhibitor of NF-κB, abolished growth of resistant cells; however, the possibility that inhibition of additional targets by dexamethasone contributed to EGCG sensitivity has not been excluded. Importantly, expression profiling of the original and resistant NF639 cells followed by GSEA pathway analysis revealed that MAPK is more highly activated in the resistant cells. Consistent with this analysis, resistant cells were more sensitive to the MAPK inhibitor U0216 and the combined treatment of EGCG and U0216 appeared to effectively revert mesenchymal phenotype. Thus, GSEA was useful in identifying aberrantly activated pathways (e.g., MAPK) that sustains a more transformed phenotype. Targeting of these pathways effectively reduced transformed phenotype. The appearance of EGCG-resistant cells after initial growth inhibition is reminiscent of the resistance emerging with other Her-2/neu–targeting methods (14, 17). Although gene profiling to assess treatment regimens has become an almost standard procedure, our findings suggest that use of pathway analysis may provide for a more rational design of effective systemic therapeutic regimens for patients whose cancers have developed drug resistance.

The 67 kDa laminin receptor (67LR) was reported as a receptor for EGCG, and ectopic expression of 67LR conferred EGCG sensitivity to cells (37). However, whereas we found an ~2-fold reduction in 67LR protein in resistant lines or upon EGCG treatment, ectopic expression of the cDNA encoding the 37 kDa precursor protein in the original population was unable to enhance the sensitivity to EGCG (data not shown). This may be due to the failure to process the mature form of 67LR in these cells, or, alternatively, the 67LR pathway might not be a prevalent mechanism in our experimental setting. Furthermore, the CCN family of growth factor Wnt signaling induced secreted protein 1 (WISP-1), which promotes survival by attenuating p53-mediated apoptosis (38), was found to be increased ~2- to 3-fold as judged by reverse transcription-PCR in the resistant cells; however, ectopic expression of WISP-1 in NF639 cells did not alter their sensitivity to EGCG (data not shown). Very recently, EGCG has been found to

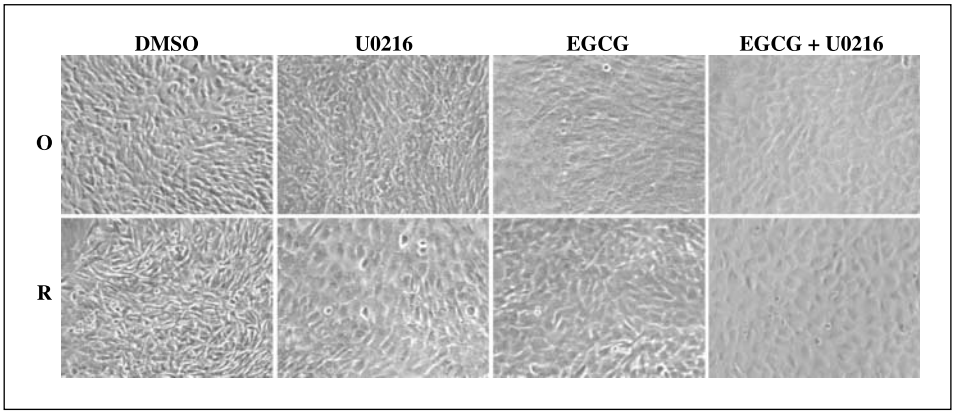

Figure 5. Combined treatment of EGCG and U0216 MAPK inhibitor reduces mesenchymal phenotype. Original and resistant populations of cells were plated at 10,000 per well in a 12-well dish. On the following day, cells were treated with either 20 μmol/L U0216 or 40 μg/mL EGCG alone or in combination, as indicated. After 72 hours of treatment, cells were photographed and representative fields are shown.

associate with vimentin (39), a protein that is more highly expressed in mesenchymal cells (40). The *vimentin* gene is also a known NF-κB target gene (41). Sensitivity to the chemopreventive effects of green tea polyphenols has been studied in human populations and the effectiveness of green tea has been related to genetic background. In particular, two genetic loci have been reported to control the response to tea polyphenols. In human populations, the catechol-*O*-methyltransferase (*COMT*) allele is polymorphic and an individual can inherit either none, one, or two copies of an allele that encodes an enzyme with higher activity. COMT is involved in the rapid biotransformation and elimination of tea catechins after ingestion (42). The association between tea consumption and breast cancer risk reduction could be observed only among individuals who possessed at least one copy of the low-activity *COMT* allele (43). Another genetic locus shown to affect the responsiveness to green tea is glutathione *S*-transferase, a member of the phase II group of xenobiotic metabolizing enzymes. When the effects of high consumption (4 cups/d) of green tea or black tea on cigarette smoking induced oxidative DNA damage were studied, only the *GSTM1*-positive and *GSTT1*-positive smokers showed a statistically significant decrease in urinary 8-OHdG level, a marker of DNA damage, after 4 months of drinking green tea (44). The new field of nutrigenomics proposes to examine the expression profiles of cells from individuals with different genetic backgrounds to help design personalized chemopreventive and chemotherapeutic strategies.

Here, we show that the combination of EGCG and either dexamethasone or U0216 more effectively reduced transformed phenotype of Her-2/neu–driven cancer cells. Several groups have shown that antimetabolites in cancer chemotherapy can be more effective in animal and cell culture models when used in combination with green tea extracts. Green tea extracts enhanced the cytotoxicity of cytosine arabinoside and methotrexate (45). A combination of EGCG and dacarbazine was more effective than EGCG alone in reducing the number of pulmonary metastases and primary tumor growths, and increasing the survival rate of melanoma-bearing mice (46). EGCG induced tumor cell apoptosis synergistically with sulindac and tamoxifen in the human lung cancer cell line PC-9 and in the intestinal tumors in multiple intestinal neoplasia (Min) mice (47, 48). This may be due in part to the effects of tea components on uptake. Powdered green tea significantly enhanced mitomycin C uptake in Ehrlich ascites carcinoma cells (49). The injection of doxorubicin alone did not inhibit M5076 tumor growth in mice, whereas the combination of the tea derivative theanine and doxorubicin significantly reduced the tumor weight. Importantly, an increase in effectiveness may allow for a reduction in dose of a chemotherapeutic agent, thereby reducing deleterious side effects. For example, the combination of EGCG and curcumin allowed for a dose reduction of 4.4- to 8.5-fold for EGCG and 2.2- to 2.8-fold for curcumin (50). It is important to assess whether the green tea polyphenol EGCG can be used in combinatorial treatments to enhance the effectiveness of therapeutic regimens in the clinic.

Acknowledgments

Received 12/1/2005; revised 2/1/2006; accepted 3/3/2006.

Grant support: NIH grant PO1 ES11624.

The costs of publication of this article were defrayed in part by the payment of page charges. This article must therefore be hereby marked *advertisement* in accordance with 18 U.S.C. Section 1734 solely to indicate this fact.

We thank Dr. M. Panchenko for providing U0216 and for helpful discussions; P. Leder for the NF639 cell line; and Drs. K. Ravid, K. Symes, and K. Kirsch for assistance with the photography.

References

1. Hortobagyi GN, Hung MC, Buzdar AU. Recent developments in breast cancer therapy. Semin Oncol 1999;26:11–20.
2. Eccles SA. The role of c-erbB-2/HER2/neu in breast cancer progression and metastasis. J Mammary Gland Biol Neoplasia 2001;6:393–406.
3. Guy CT, Webster MA, Schaller M, et al. Expression of the neu protooncogene in the mammary epithelium of transgenic mice induces metastatic disease. Proc Natl Acad Sci U S A 1992;89:10578–82.
4. Zhou BP, Hung MC. Dysregulation of cellular signaling by HER2/neu in breast cancer. Semin Oncol 2003;30:38–48.
5. Schiff R, Massarweh S, Shou J, Osborne CK. Breast cancer endocrine resistance: how growth factor signaling and estrogen receptor coregulators modulate response. Clin Cancer Res 2003;9:447–54S.
6. Hung MC, Lau YK. Basic science of HER-2/neu: a review. Semin Oncol 1999;26:51–9.
7. Pianetti S, Arsura M, Romieu-Mourez R, Coffey RJ, Sonenshein GE. Her-2/neu overexpression induces NF-κB via a PI3-kinase/Akt pathway involving calpain-mediated degradation of IκB-α that can be inhibited by the tumor suppressor PTEN. Oncogene 2001;20:1287–99.
8. Sovak MA, Bellas RE, Kim DW, et al. Aberrant nuclear factor-κB/Rel expression and the pathogenesis of breast cancer. J Clin Invest 1997;100:2952–60.
9. Romieu-Mourez R, Kim DW, Shin SM, et al. Mouse mammary tumor virus c-rel transgenic mice develop mammary tumors. Mol Cell Biol 2003;23:5738–54.
10. Wu M, Lee H, Bellas RE, et al. Inhibition of NF-κB/Rel induces apoptosis of murine B cells. EMBO J 1996;15:4682–90.
11. Baldwin AS. Control of oncogenesis and cancer therapy resistance by the transcription factor NF-κB. J Clin Invest 2001;107:241–6.
12. Muerkoster S, Arlt A, Witt M, et al. Usage of the NF-κB inhibitor sulfasalazine as sensitizing agent in combined chemotherapy of pancreatic cancer. Int J Cancer 2003;104:469–76.
13. Pommier Y, Sordet O, Antony S, Hayward RL, Kohn KW. Apoptosis defects and chemotherapy resistance: molecular interaction maps and networks. Oncogene 2004;23:2934–49.
14. Baselga J. Clinical trials of Herceptin (trastuzumab). Eur J Cancer 2001;37 Suppl 1:S18–24.
15. Slamon DJ, Leyland-Jones B, Shak S, et al. Use of chemotherapy plus a monoclonal antibody against HER2 for metastatic breast cancer that overexpresses HER2. N Engl J Med 2001;344:783–92.
16. Kurata T, Tamura K, Kaneda H, et al. Effect of re-treatment with gefitinib ("Iressa", ZD1839) after acquisition of resistance. Ann Oncol 2004;15:173–4.
17. Li B, Chang CM, Yuan M, McKenna WG, Shu HK. Resistance to small molecule inhibitors of epidermal growth factor receptor in malignant gliomas. Cancer Res 2003;63:7443–50.
18. Kunitomo K, Inoue S, Ichihara F, et al. A case of metastatic breast cancer with outgrowth of HER2-negative cells after eradication of HER2-positive cells by humanized anti-HER2 monoclonal antibody (trastuzumab) combined with docetaxel. Hum Pathol 2004;35:379–81.
19. Guo S, Sonenshein GE. Mechanisms of green tea action. In: Kaput J, Rodriguez RL, editors. Nutritional genomics: discovering the path to personalized nutrition. Hoboken, NJ: John Wiley & Sons, Inc.; 2006. p. 177–206.
20. Dreosti IE, Wargovich MJ, Yang CS. Inhibition of carcinogenesis by tea: the evidence from experimental studies. Crit Rev Food Sci Nutr 1997;37:761–70.
21. Kavanagh KT, Hafer LJ, Kim DW, et al. Green tea extracts decrease carcinogen-induced mammary tumor burden in rats and rate of breast cancer cell proliferation in culture. J Cell Biochem 2001;82:387–98.
22. Pianetti S, Guo S, Kavanagh KT, Sonenshein GE. Green tea polyphenol epigallocatechin-3 gallate inhibits Her-2/neu signaling, proliferation, and transformed phenotype of breast cancer cells. Cancer Res 2002;62:652–5.
23. Elson A, Leder P. Protein-tyrosine phosphatase epsilon. An isoform specifically expressed in mouse mammary tumors initiated by v-Ha-ras OR neu. J Biol Chem 1995;270:26116–22.
24. Duyao MP, Buckler AJ, Sonenshein GE. Interaction of an NF-κB-like factor with a site upstream of the c-myc promoter. Proc Natl Acad Sci U S A 1990;87:4727–31.
25. Jiang HY, Petrovas C, Sonenshein GE. RelB-p50 NF-κB complexes are selectively induced by cytomegalovirus immediate-early protein 1: differential regulation of Bcl-x(L) promoter activity by NF-κB family members. J Virol 2002;76:5737–47.
26. Subramanian A, Tamayo P, Mootha VK, et al. From the cover: gene set enrichment analysis: a knowledge-based approach for interpreting genome-wide expression profiles. Proc Natl Acad Sci U S A 2005;102:15545–50.
27. Ignatoski KM, Maehama T, Markwart SM, et al. ERBB-2 overexpression confers PI3′ kinase-dependent invasion capacity on human mammary epithelial cells. Br J Cancer 2000;82:666–74.
28. Ozes ON, Mayo LD, Gustin JA, et al. NF-κB activation by tumour necrosis factor requires the Akt serine-threonine kinase. Nature 1999;401:82–5.
29. Rawadi G, Garcia J, Lemercier B, Roman-Roman S. Signal transduction pathways involved in the activation

of NF-κ B, AP-1, and c-fos by *Mycoplasma fermentans* membrane lipoproteins in macrophages. J Immunol 1999;162:2193–203.
30. Thompson JE, Phillips RJ, Erdjument-Bromage H, Tempst P, Ghosh S. IκB-β regulates the persistent response in a biphasic activation of NF-κB. Cell 1995;80:573–82.
31. Jeay S, Pianetti S, Kagan HM, Sonenshein GE. Lysyl oxidase inhibits ras-mediated transformation by preventing activation of NF-κB. Mol Cell Biol 2003;23:2251–63.
32. Scheinman RI, Gualberto A, Jewell CM, Cidlowski JA, Baldwin AS, Jr. Characterization of mechanisms involved in transrepression of NF-κ B by activated glucocorticoid receptors. Mol Cell Biol 1995;15:943–53.
33. Thiery JP. Epithelial-mesenchymal transitions in tumour progression. Nat Rev Cancer 2002;2:442–54.
34. Lu Z, Xu S, Joazeiro C, Cobb MH, Hunter T. The PHD domain of MEKK1 acts as an E3 ubiquitin ligase and mediates ubiquitination and degradation of ERK1/2. Mol Cell 2002;9:945–56.
35. Silletti S, Yebra M, Perez B, et al. Extracellular signal-regulated kinase (ERK)-dependent gene expression contributes to L1 cell adhesion molecule-dependent motility and invasion. J Biol Chem 2004;279:28880–8.
36. Klemke RL, Cai S, Giannini AL, et al. Regulation of cell motility by mitogen-activated protein kinase. J Cell Biol 1997;137:481–92.
37. Tachibana H, Koga K, Fujimura Y, Yamada K. A receptor for green tea polyphenol EGCG. Nat Struct Mol Biol 2004;11:380–1.
38. Su F, Overholtzer M, Besser D, Levine AJ. WISP-1 attenuates p53-mediated apoptosis in response to DNA damage through activation of the Akt kinase. Genes Dev 2002;16:46–57.
39. Ermakova S, Choi BY, Choi HS, et al. The intermediate filament protein vimentin is a new target for epigallocatechin gallate. J Biol Chem 2005;280:16882–90.
40. Lane EB, Hogan BL, Kurkinen M, Garrels JI. Co-expression of vimentin and cytokeratins in parietal endoderm cells of early mouse embryo. Nature 1983;303:701–4.
41. Lilienbaum A, Paulin D. Activation of the human vimentin gene by the Tax human T-cell leukemia virus. I. Mechanisms of regulation by the NF-κB transcription factor. J Biol Chem 1993;268:2180–8.
42. Lu H, Meng X, Yang CS. Enzymology of methylation of tea catechins and inhibition of catechol-*O*-methyltransferase by (−)-epigallocatechin gallate. Drug Metab Dispos 2003;31:572–9.
43. Wu AH, Tseng CC, Van Den Berg D, Yu MC. Tea intake, COMT genotype, and breast cancer in Asian-American women. Cancer Res 2003;63:7526–9.
44. Hakim IA, Harris RB, Chow HH, et al. Effect of a 4-month tea intervention on oxidative DNA damage among heavy smokers: role of glutathione *S*-transferase genotypes. Cancer Epidemiol Biomarkers Prev 2004;13:242–9.
45. Zhen Y, Cao S, Xue Y, Wu S. Green tea extract inhibits nucleoside transport and potentiates the antitumor effect of antimetabolites. Chin Med Sci J 1991;6:1–5.
46. Liu JD, Chen SH, Lin CL, Tsai SH, Liang YC. Inhibition of melanoma growth and metastasis by combination with (−)-epigallocatechin-3-gallate and dacarbazine in mice. J Cell Biochem 2001;83:631–42.
47. Suganuma M, Okabe S, Kai Y, et al. Synergistic effects of (−)-epigallocatechin gallate with (−)-epicatechin, sulindac, or tamoxifen on cancer-preventive activity in the human lung cancer cell line PC-9. Cancer Res 1999;59:44–7.
48. Suganuma M, Ohkura Y, Okabe S, Fujiki H. Combination cancer chemoprevention with green tea extract and sulindac shown in intestinal tumor formation in Min mice. J Cancer Res Clin Oncol 2001;127:69–72.
49. Kurita T, Miyagishima A, Nozawa Y, Sadzuka Y, Sonobe T. A dosage design of mitomycin C tablets containing finely powdered green tea. Int J Pharm 2004;275:279–83.
50. Khafif A, Schantz SP, Chou TC, Edelstein D, Sacks PG. Quantitation of chemopreventive synergism between (−)-epigallocatechin-3-gallate and curcumin in normal, premalignant and malignant human oral epithelial cells. Carcinogenesis 1998;19:419–24.